Since January 2020 Elsevier has created a COVID-19 resource centre with free information in English and Mandarin on the novel coronavirus COVID-19. The COVID-19 resource centre is hosted on Elsevier Connect, the company's public news and information website.

Cell Insight 1 (2022) 100046

Contents lists available at ScienceDirect

Cell Insight

journal homepage: www.journals.elsevier.com/cell-insight

Screening of SARS-CoV-2 antivirals through a cell-based RNA-dependent RNA polymerase (RdRp) reporter assay

Timsy Uppal [a], Kai Tuffo [a], Svetlana Khaiboullina [a], Sivani Reganti [a], Mark Pandori [b], Subhash C. Verma [a,*]

[a] Department of Microbiology and Immunology, University of Nevada, Reno, NV, 89557, USA
[b] Nevada State Public Health Laboratory, Reno, NV, 89557, USA

HIGHLIGHTS

- We have developed a robust high-throughput cell-based assay for screening anti-SARS-CoV-2 anti-virals.
- Dasabuvir inhibited the RNA-dependent RNA polymerase of SARS-CoV-2 and reduced the production of cell-free viruses.
- The replication assay showed inhibition of SARS-CoV-2 variants, USA-WA1/2020, and B.1.617.2 by dasabuvir at similar EC_{50}.

GRAPHICAL ABSTRACT

Cell-based reporter assay for screening SARS-CoV-2 RdRp inhibitors. Anti-virals capable of blocking the RdRp activity or working as nucleosi(ti)de analog reduce the levels of reporter genes and the production of cell-free viruses.

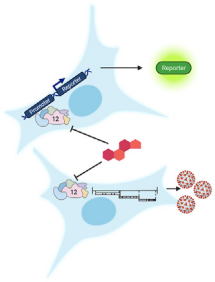

ARTICLE INFO

Keywords:
SARS-CoV-2
COVID-19
RdRp
Antivirals
Dasabuvir
Ribavirin
FDA

ABSTRACT

COVID-19 (Coronavirus Disease 2019) caused by SARS-CoV-2 (Severe Acute Respiratory Syndrome CoronaVirus-2) continues to pose an international public health threat and thus far, has resulted in greater than 6.4 million deaths worldwide. Vaccines are critical tools to limit COVID-19 spread, but antiviral drug development is an ongoing global priority due to fast-spreading COVID-19 variants that may elude vaccine efficacies. The RNA-dependent RNA polymerase (RdRp) of SARS-CoV-2 is an essential enzyme of viral replication and transcription machinery complex. Therefore, the RdRp is an attractive target for the development of effective anti-COVID-19 therapeutics. In this study, we developed a cell-based assay to determine the enzymatic activity of SARS-CoV-2 RdRp through a luciferase reporter system. The SARS-CoV-2 RdRp reporter assay was validated using known inhibitors of RdRp polymerase, remdesivir along with other anti-virals including ribavirin, penciclovir, rhoifolin, 5′CT, and dasabuvir. Dasabuvir (an FDA-approved drug) exhibited promising RdRp inhibitory activity among these inhibitors. Anti-viral activity of dasabuvir was also tested on the replication of SARS-CoV-2 through infection of Vero E6 cells. Dasabuvir inhibited the replication of SARS-CoV-2, USA-WA1/2020 as well as B.1.617.2 (delta variant) in Vero E6 cells in a dose-dependent manner with EC_{50} values 9.47 μM and 10.48 μM, for USA-WA1/2020 and B.1.617.2 variants, respectively. Our results suggest that dasabuvir can be further evaluated as a therapeutic drug for COVID-19. Importantly, this system provides a robust, target-specific, and high-

* Corresponding author.
E-mail address: scverma@med.unr.edu (S.C. Verma).

https://doi.org/10.1016/j.cellin.2022.100046
Received 9 May 2022; Received in revised form 24 June 2022; Accepted 25 June 2022
Available online 29 June 2022

throughput screening compatible (z- and z'-factors of >0.5) platforms that will be a valuable tool for screening SARS-CoV-2 RdRp inhibitors.

1. Introduction

The life-threatening COVID-19 is caused by SARS-CoV-2, a new coronavirus discovered in 2019, which caused a global pandemic (Wang et al., 2020). SARS-CoV-2 belongs to the *betacoronavirus* genus, together with SARS-CoV and MERS-CoV, and has a high potential to cause lethal zoonotic infections among existing human coronaviruses/HCoVs (Dhama et al., 2020). SARS-CoV-2 mainly attacks the lower respiratory system to cause pneumonia-like symptoms, but can also damage the digestive system, gastrointestinal system, heart, kidney, liver, and central nervous system leading to multiple organ failure and death in severe COVID-19 patients (Mokhtari et al., 2020). Extensive efforts are being made worldwide to develop efficacious antiviral drugs against COVID-19 infections.

SARS-CoV-2 is an enveloped, positive-sense single-stranded RNA virus. The polycistronic RNA genome (~30 kb) has 14 open reading frames (ORFs) that encode two groups of proteins (Romano et al., 2020). Approximately, one-third of the SARS-CoV-2 genome encodes for four structural proteins [spike (**S**), envelope I, membrane (**M**), and nucleocapsid (**N**)] and six accessory proteins, encoded by ORFs 2–10 (Naqvi et al., 2020). The remaining two-thirds of the viral genome encodes for non-structural proteins, expressed as two large replicase polyproteins (ORF1a and ORF1ab), which are cleaved by the virus's proteases, M^{pro} and $PL^{pro,}$ into 16 small peptides, nsp1-16. The replicative proteins assemble into a membrane-bound ribonucleoprotein complex (or replication and transcription complex) that directs RNA synthesis and processing. Several proteins of the nsp interactome thus serve as potential targets for developing the antiviral (Liu et al., 2021). The RNA-dependent RNA polymerase (RdRp), one of the SARS-CoV-2 non-structural proteins (nsp12), is the central catalytic subunit of the viral RNA synthesizing machinery (Gao et al., 2020). RdRp's crucial role in the virus replication and absence of closely related homolog in humans makes it an important druggable molecular target of SARS-CoV-2 inhibition.

Hillen et al. recently resolved the structure of replicating SARS-CoV-2 RdRp polymerase in its active form using a cryo-electron microscopy (Hillen et al., 2020). Similar to RdRp of SARS, SARS-CoV-2 RdRp also consists of a catalytic domain of nsp12, one copy of nsp7, two copies of nsp8, and more than two turns of RNA template-product duplexes. As a result, known inhibitors of RdRp of SARS might show promising effects against RdRp of SARS-CoV-2. A wide array of adenine and guanine-based nucleoside analog inhibitors targeting viral RdRp polymerase have been considered against SARS-CoV-2 (Chien et al., 2020; Vicenti et al., 2021). However, only a few anti-virals, remdesivir (GS-5734) by Gilead Sciences, molnupiravir by Merck, and paxlovid by Pfizer, are authorized for emergency use in treating mild to moderate COVID-19 infection (Anastassopoulou et al., 2022). These drugs are shown to inhibit SARS, MERS, and SARS-CoV-2 replication in cell culture and animal models by either targeting the RdRp (Gordon et al., 2020; Williamson et al., 2020; Kabinger et al., 2021; Kokic et al., 2021) or M^{pro} main protease (Owen et al., 2021). Since, HCoVs encode a protein (nsp14) with exonuclease activity, for proofreading through the removal of incorrect bases, nucleos(t)ide analogs (NAs) may become ineffective, thus necessitating the development of anti-virals capable of blocking the enzymatic activity of the RdRp, along with identifying NAs for blocking the RNA synthesis.

Identification of inhibitors through high-throughput screening (HTS) requires a cost-efficient, robust, convenient-to-use, and highly reliable assay. To improve the current efforts in finding SARS-CoV-2 antivirals, especially RdRp-specific inhibitors, we developed a HEK293 cell-based stable RdRp reporter assay capable of specifically monitoring SARS-CoV-2 RdRp polymerase activity in cellular conditions. The SARS-CoV-2 RdRp reporter was developed by modifying the reporter systems reported for HCV NS5B, and MERS-CoV (Lee et al., 2010; Min et al., 2020). The use of in-built control monitoring RdRp polymerase activity allows the identification of selective RdRp inhibitors in a single assay. We evaluated the inhibitory effect of known RdRp inhibitors, i.e., rhoifolin, dasabuvir, ribavirin, penciclovir, and cytidine-5'triphosphate in our cell-based reporter assay, which identified dasabuvir as a potent inhibitor of SARS-CoV-2 RdRp activity. Furthermore, the inhibitory activity of dasabuvir was validated in an infection assay with two different SARS-CoV-2 (USA-WA1/2020 and B.1.617.2) variants. These results demonstrate that our cells-based assay can be used for screening compounds capable of blocking the RdRp activity of SARS-CoV-2.

2. Results

2.1. Development of cell-based SARS-CoV-2 RdRp reporter assay

In order to measure the intracellular SARS-CoV-2 RdRp (nsp12)

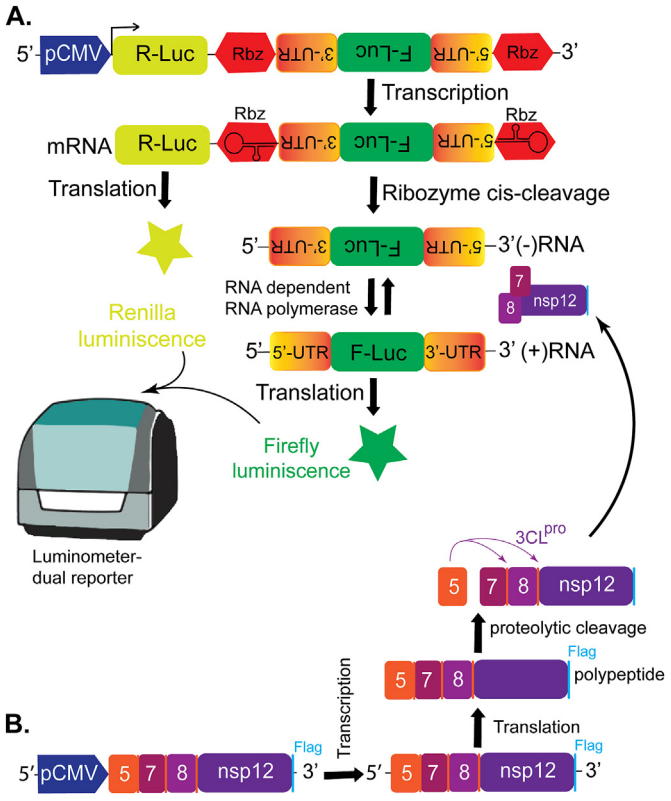

Fig. 1. Cell-based SARS-CoV-2 RdRp Activity Reporter. A) Schematic diagram of the bicistronic SARS-CoV-2 RdRp reporter construct p(+)RLuc-(−)UTR-FLuc.The construct contains the *renilla* luciferase (RLuc) gene cloned in a positive direction under CMV promoter, and the *firefly* luciferase (FLuc) gene under the control of the 5′-untranslated region (UTR). FLuc gene is flanked by 5′-UTR and 3′-UTR of SARS-CoV-2 and the hepatitis delta virus (HDV) ribozyme self-cleavage sequence. RLuc serves as an internal control to normalize FLuc activity. Expression of RdRp in trans will control FLuc levels and compounds/mutations altering RdRp activity will be reflected by a reduction in FLuc levels. (B) Schematic representation of the plasmid construct expressing SARS-CoV-2 RdRp (nsp12), accessory proteins (nsp7, and nsp8), and viral $3CL^{pro}$ protease (nsp5), required for proper cleavage of the proteins. Cleavage of the proteins is confirmed by the expression of flag-tagged nsp12 (RdRp) in an immunoblotting assay.

enzymatic activity, we developed a cell-based luciferase reporter system, using a similar principle as reported earlier for cell-based HCV RdRp and MERS-CoV RdRp activity assays (Lee et al., 2010; Min et al., 2020). The schematic of the bicistronic SARS-CoV-2 RdRp reporter constructs used in the system, with firefly luciferase (FLuc) and renilla luciferase (RLuc) genes in reverse orientation, designated as p(+)RLuc-(−)UTR-FLuc is shown in Fig. 1A. The (−)FLuc is flanked by the 5′-UTR and 3′-UTR of SARS-CoV-2 and ribozyme self-cleavage sequence of the hepatitis delta virus (HDV). The transcription of full length (+)RLuc-(−)UTR-FLuc RNA is catalyzed by the host RNA polymerase Pol II. The generated bicistronic RNA transcripts are further self-cleaved by the ribozyme, leading to the expression of FLuc RNA in a negative-sense orientation, that is, then transcribed to a positive-sense FLuc RNA by RdRp polymerase for protein synthesis. Thus, the intensity of the measured FLuc signal is proportional to the level of intracellular RdRp polymerase activity. In addition, in the presence of RdRp activity, the amounts of synthesized (+) Fluc RNA gets amplified, whereas the levels of RLuc RNA (serving as an internal control of transcription and translation) remain unaffected. To transiently express SARS-CoV-2 RdRp in mammalian cells, we constructed a Flag-tagged nsp5, 7, 8,12 vector as shown in Fig. 1B. The construct expressed RdRp as a polypeptide with other accessory proteins, namely nsp7, nsp8 (accessory proteins for the RdRp activity), and $3CL^{pro}$ (nsp5, with autoproteolytic activity). A flag tag introduced at the 3'end of nsp12 (RdRp) helped in determining the expression and cleavage from the polypeptide.

2.2. Determination of SARS-CoV-2 RdRp polymerase activity

To test our SARS-CoV-2 RdRp reporter system and the activity of intracellular SARS-CoV-2 RdRp, we co-transfected RdRp-reporter construct with pcDNA3.1 (control) or varying amounts (1 μg and 3 μg) of Flag-tagged nsp5,7,8,12 expressing plasmid in HEK293 cells. At 48h post-transfection, we tested the expression of flag-tagged SARS-CoV-2 RdRp in the cells by western blotting with an anti-flag antibody, along with anti-GAPDH for the loading control (Fig. 2A). A dose-dependent increase in the RdRp protein expression was observed in the cells as confirmed by bands at 110 kDa. The absence of a corresponding band in the cells transfected with an empty vector confirmed the expression of Rdp. The dose-dependent increase in the FLuc and FLuc/RLuc levels is expected to be proportional to the increase in amounts of (+) FLuc RNA transcripts, which is dependent on RdRp polymerase activity. In order to confirm this, we performed a dual-luciferase reporter assay and rt-qPCR on HEK293 cells co-transfected with the above combination of plasmids. As seen in Fig. 2B, both the FLuc and the relative FLuc (Index value) levels were increased by the expression of flag-tagged SARS-CoV-2 RdRp in a dose-dependent manner, while the increase in RLuc level wasn't changed as much. The rt-qPCR using primers specific to the FLuc and RLuc genes, with beta-actin as the internal control, showed an increase in the FLuc mRNA expression level. In addition, an increase in the relative FLuc/RLuc mRNA expression levels was directly proportional to increased amounts of Flag-tagged RdRp present in HEK293 cells (Fig. 2C). No significant increase in the levels of RLuc RNA was observed for the transfected cells, confirming that RdRp did not affect the levels of RLuc, as expected.

2.3. Generation and characterization of HEK293 cells stably expressing SARS-CoV-2 RdRp reporter construct

Since the FLuc levels, indirectly measuring the RdRp activity, was significantly enhanced in the transient assay described above, we generated HEK293 cells stably expressing SARS-CoV-2 RdRp reporter and pcDNA3.1 (control) or Flag-tagged nsp5, 7, 8, and 12 polypeptides by co-transfecting RdRp-reporter with either pcDNA3.1 or Flag-tagged nsp5, 7, 8, 12 expression constructs. The stable expression of RdRp polymerase aids in the development of a reporter system for a high-throughput screening (HTS) platform. Transfected cells were selected

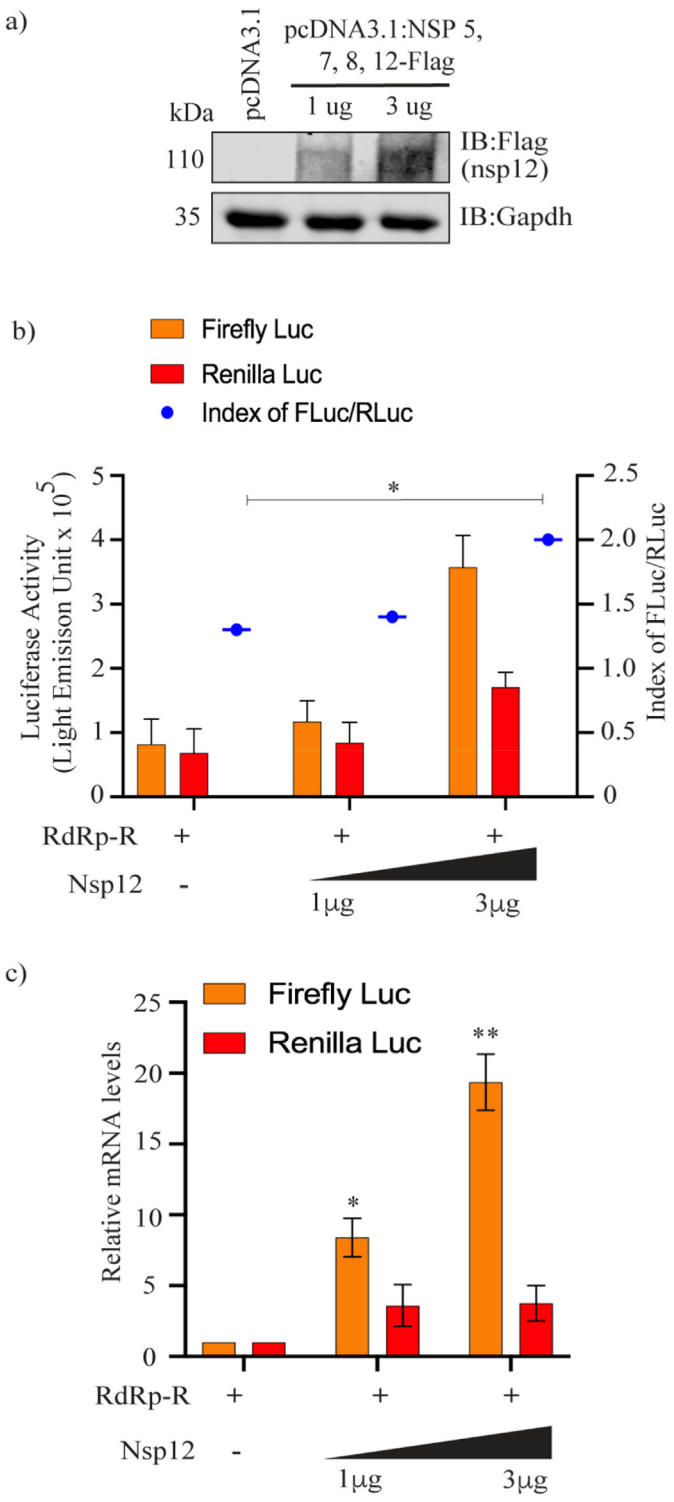

Fig. 2. Transient reporter assay of SARS-CoV-2 RdRp polymerase. (A) Transiently transfected cells were subjected to immunoblotting with anti-flag (nsp12) and GAPDH antibodies at 48h post-transfection. (B) HEK293L cells expressing SARS-CoV-2 RdRp reporter (Rdzrp-R) with either control pcDNA3.1 or Flag-tagged nsp5,7,8,12 (Nsp12) construct were subjected to luminescence detection with the dual-luciferase reporter assay 48hpt, and the FLuc, Rluc, and ratio of FLuc/RLuc (Index) levels were determined. (C) Total RNA was extracted, and FLuc mRNA and RLuc mRNA expression levels were assayed by RT-qPCR. Statistical significance *, $p < 0.1$; and **, $p < 0.01$.

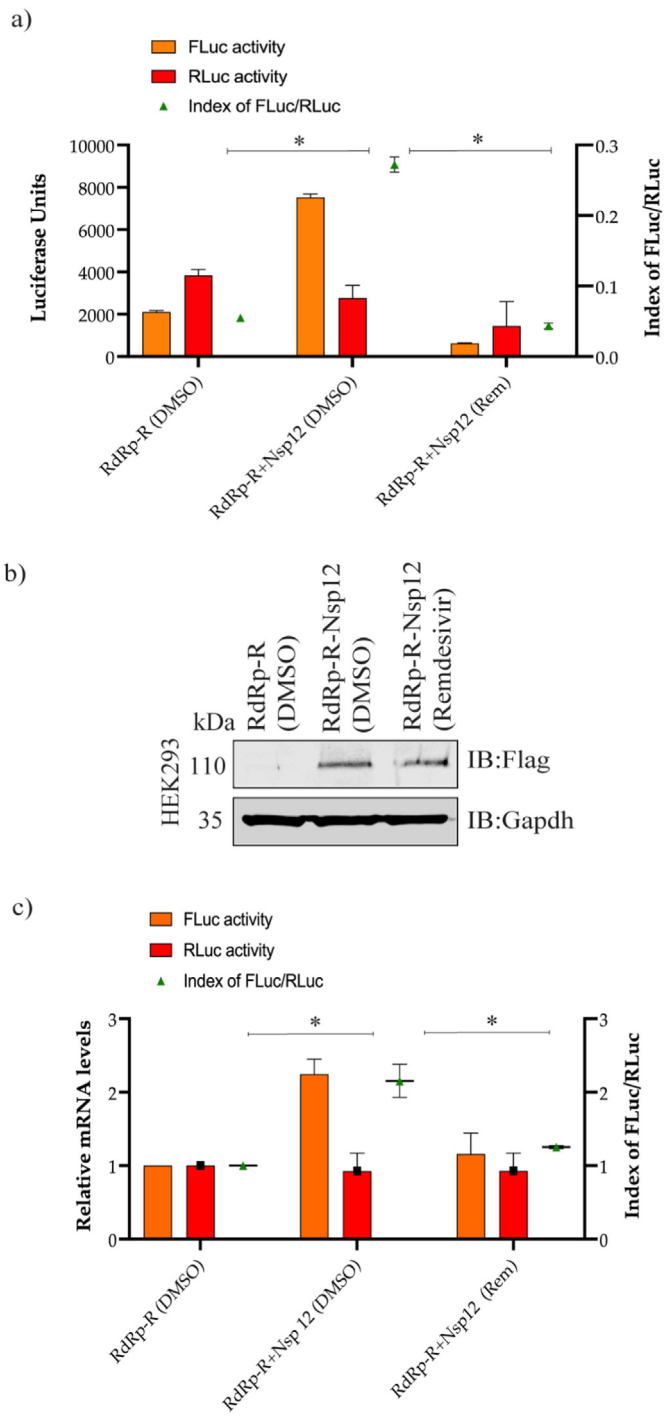

Fig. 3. Characterization of 293 cells stably expressing SARS-CoV-2 RdRp reporter. (A) Cells stably expressing the SARS-CoV-2 RdRp reporter and pcDNA3.1 or Flag-tagged nsp5,7,8, and 12 constructs were mock (DMSO) treated or treated with remdesivir (a potent anti-RdRp inhibitor), followed by luminescence detection with the dual-luciferase reporter assay, and the relative FLuc/RLuc ratio (Index) was detected after 48h. (B) Cells were also subjected to immunoblotting with anti-flag antibody 48h post-transfection, and (C) Total RNA was extracted and relative FLuc/RLuc RNA expression levels were quantified by RT-qPCR, using luciferase gene-specific primers and beta-actin, as an internal control. Statistical significance *, $p < 0.1$.

with 250 μg/mL G418 (293-RdRp cells) or 250 μg/mL G418 and 25 μg/mL hygromycin (293-RdRp-nsp5,7,8,12-flag cells) at 24h post-transfection. After 3-weeks of selection, cells were analyzed for luminometric activity using the dual-luciferase reporter assay kit (Fig. 3A), and RdRp protein expression by an immunoblotting assay using an anti-flag antibody (Fig. 3B). For the reporter assay, an equal number of 293-RdRp and 293-RdRp-nsp5, 7, 8,12-flag cells were treated with DMSO for 48h and assayed with dual-luciferase reporter assay. In addition, we treated an equal number of 293-RdRp-nsp5, 7, 8,12-flag cells with remdesivir, a known SARS-CoV-2 RdRp inhibitor, to further validate our reporter system. As seen in Fig. 3A, the calculated FLuc/RLuc ratio (Index value) in the cells constitutively expressing RdRp reporter and the polypeptide, was higher (Fig. 3A, RdRp Nsp-DMSO bars) than in cells harboring RdRp reporter without the nsp5, 7, 8,12-flag (Fig. 3A, RdRp-DMSO bars). Importantly, the addition of remdesivir reduced the levels of FLuc or relative FLuc/RLuc ratios (index value), with respect to the DMSO-treated set (Fig. 3A, RdRp Nsp-Rem bars), as expected. Western blot analysis of these cells confirmed the expression of flag-tagged SARS-CoV-2 RdRp protein, indicated by the appearance of the expected size band at 110 kDa (Fig. 3B) in 293-RdRp-nsp5,7,8,12-flag cells (mock-as well as remdesivir treated sets). 293-RdRp reporter cells lacked the detection of RdRp protein, as expected. Relative quantification of the bicistronic genes (FLuc and RLuc) copy number from stable cells was performed using quantitative rt-PCR with primers corresponding to the FLuc gene and RLuc, with levels of the cellular β-*actin* gene as the normalization control. The increase in FLuc levels in the 293 cells, constitutively expressing SARS-CoV-2 RdRp reporter and Flag-tagged RdRp protein was proportional to the increase in the mRNA levels of (+) FLuc (generated by RdRp), as compared to RdRp reporter cells lacking RdRp expression (Fig. 3C, lane 1 and 2). The levels of (+) FLuc RNAs were also quantified after treatment with remdesivir. As seen in Fig. 3C, treatment with RdRp inhibitor significantly reduced the mRNA levels of (+) FLuc. This confirmed that this cell-based reporter system can be used to quantitatively assess the intracellular SARS-CoV-2 RdRp activity.

2.4. *Evaluation of reporter assay system for high-throughput screening (HTS) of SARS-CoV-2 RdRp inhibitors*

To determine if the cell-based reporter assay is suitable for HTS applications, we calculated screening window coefficients, Z-, and Z′-factors using Zhang's formulae (Sui and Wu, 2007). The Z-, and Z′-factors are widely used parameters to evaluate and validate the reliability and reproducibility of screening assay systems as HTS platforms. To calculate the screening coefficients, HEK293 cells stably expressing SARS-CoV-2 RdRp reporter system and pcDNA3.1 vector (control group) or Flag-tagged nsp5, 7, 8, and 12 vector (positive group) were treated with DMSO (0.025%) for 24h. HEK293 cells stably expressing SARS-CoV-2 RdRp reporter and Flag-tagged nsp5, 7, 8, and 12 vector were used for determining the luciferase levels without and with remdesivir (10 μM, inhibitor group) treatments for 24h through dual-luciferase reporter assay. The Z-factor (specificity of the assay for SARS-CoV-2 RdRp activity) and Z′-factor (applicability of remdesivir as a positive control), were calculated using the relative FLuc activity obtained from control and positive, and positive and inhibitor groups, respectively. We obtained Z-factor and Z′-factor values of 0.732 and 0.789 respectively, indicating the HEK293 cell-based reporter assay is excellent for assaying RdRp activity of SARS-CoV-2 and confirming the use of remdesivir as a positive control for SARS-CoV-2 RdRp specific inhibitors in HTS assays (Fig. 4). Thus, the target-specific HEK293 cell-based assay system targeting the RdRp of SARS-CoV-2 shall provide an excellent platform to facilitate the identification of efficacious SARS-CoV-2 RdRp inhibitors.

2.5. *Screening of RdRp inhibiting antivirals*

We further evaluated if the optimized SARS-CoV-2 RdRp reporter system allows for the screening of inhibitors against SARS-CoV-2 RdRp activity and virus replication *in vitro*. To this end, we determined the efficacy of commercially available viral DNA or RNA polymerase inhibitors as potential anti-virals for SARS-CoV-2, including rhoifolin,

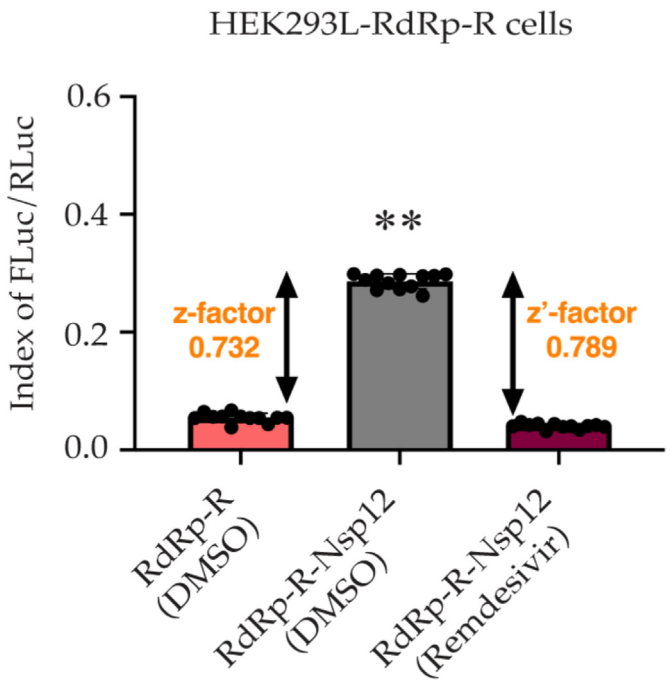

Fig. 4. Evaluation of HEK293 cell-based SARS-CoV-2 RdRp Reporter System for HTS assays. The experimental groups were characterized as: control group (n = 24)-cells expressing SARS-CoV-2 RdRp reporter and pcDNA3.1 plasmids treated with DMSO (0.025%); positive group (n = 24)-cells expressing SARS-CoV-2 RdRp reporter and Flag-tagged nsp5, 7, 8, and 12 plasmids treated with DMSO (0.025%); and inhibitor group (n = 24)-cells expressing SARS-CoV-2 RdRp reporter and Flag-tagged nsp5, 7, 8, and 12 plasmids treated with remdesivir (10 μM). The Z- and Z′-factors were calculated for HEK293 cell-based SARS-CoV-2 RdRp reporter systems, using control and positive, and positive and inhibitor groups in each 24-well plate. According to Zhang's formula, the Z-and Z'factors for HEK293 cell-based reporter assay were calculated as 0.732, and 0.789, respectively, indicating the assay system has the required robustness and reproducibility for HTS. Statistical significance **, $p < 0.01$.

ribavirin, dasabuvir, penciclovir, and cytidine-5′-triphosphate (C5′T) and DMSO (control) using our HEK293 cell-based SARS-CoV-2 RdRp reporter system. These inhibitors were added to the stable cells at a final conc. of 10 μM in medium with 10%FBS. After 48h, cells were lysed and subjected to a dual-luciferase reporter assay and FLuc/RLuc ratio (index) was determined, with the levels of FLuc activity reflecting the anti-RdRp activities of the compounds. As shown in Fig. 5A, a marked reduction in the FLuc/RLuc ratio was observed in cells treated with dasabuvir and C5′T, whereas, rhoifolin- and penciclovir-treated cells only showed a slight reduction in the FLuc/RLuc values or SARS-CoV-2 RdRp activity, with respect to the DMSO-treated cells. Interestingly, cells treated with ribavirin in combination with dasabuvir exhibited higher anti-RdRp activity when compared to cells treated with ribavirin alone.

This data confirmed that our reporter system stably expressing SARS-CoV-2 RdRp can be used for selective screening of inhibitors of SARS-CoV-2 replication within the cellular environment. In order to determine whether these antivirals have cytotoxic effects on those treated cells, which may also contribute to alter levels of FLuc/RLuc, we performed a cell viability assay using MTT analysis. This colorimetric assay provides a sensitive and accurate method for the determination of cell viability based on the generation of an insoluble formazan (purple color) from water-soluble tetrazolium MTT dye. As shown in Fig. 5B, no detectable cytotoxic effects were observed in the MTT analysis, when the cells were treated with 10 μM conc. of these selected anti-virals for 48h. Hence, this indicated that our HEK293 cell-based SARS-CoV-2 RdRp reporter system will be instrumental in screening additional novel inhibitors of SARS-CoV-2 RdRp activity.

2.6. *Effective inhibition of SARS-CoV-2 replication by dasabuvir in vitro*

We further investigated the antiviral activity of chosen compounds against SARS-CoV-2 replication *in vitro*. To this end, USA-WA1/2020 (1.6×10^6 TCID50/mL; Lot # 70036318) and B.1.617.2 (6.5×10^5 TCID50/mL[2]; Lot # 70045238) variants were obtained from BEI Resources and propagated in Vero E6 cells. Viral titers were determined after 3 days by rt-qPCR using the N1 primer-probe set. The antiviral activities of these chosen RdRp inhibitory compounds were determined

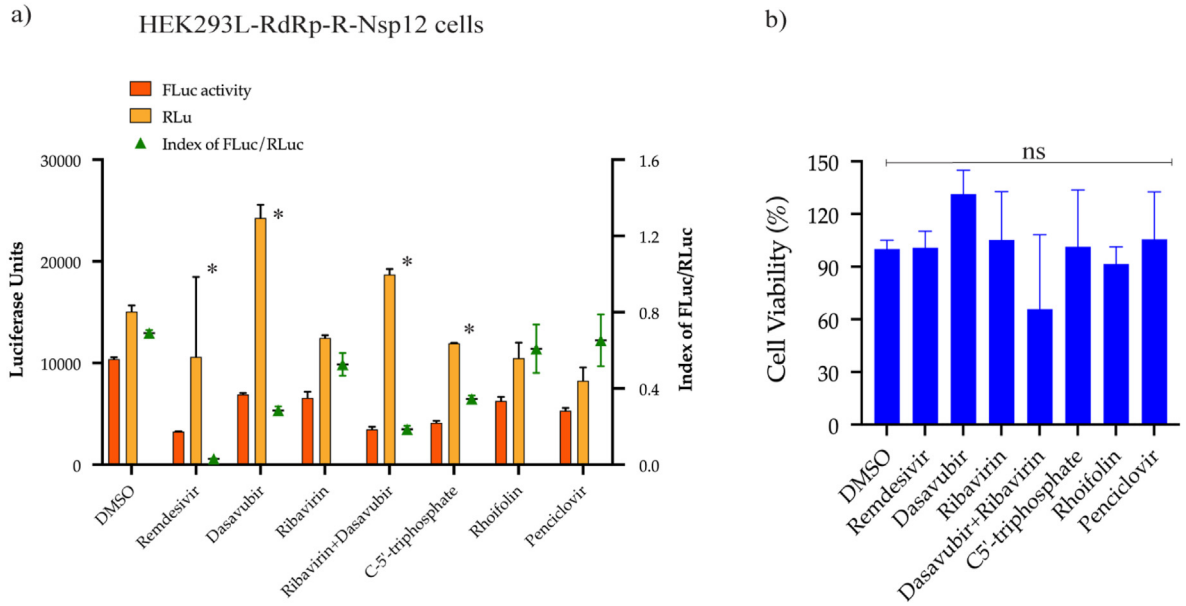

Fig. 5. Screening of the SARS-CoV-2 RdRp inhibiting compounds through a cell-based reporter system. (A) HEK293L cells with the RdRp reporter system were treated with DMSO (control) or 10 μM of test compounds and subjected to luminescence detection with the dual-luciferase reporter assay kit post 48h treatment. Firefly (FLuc) and Renilla (RLuc) luciferase values are plotted and the ratios of FLuc and RLuc (Index values), indicators of RdRp inhibition are shown. (B) The toxicity of inhibitors at 10 μM concentration on HEK293 cells was analyzed by MTT assay, 48h post-treatment. Results are presented as percent reduction with reference to DMSO from three independent experiments performed in triplicates. Statistical significance *, $p < 0.1$.

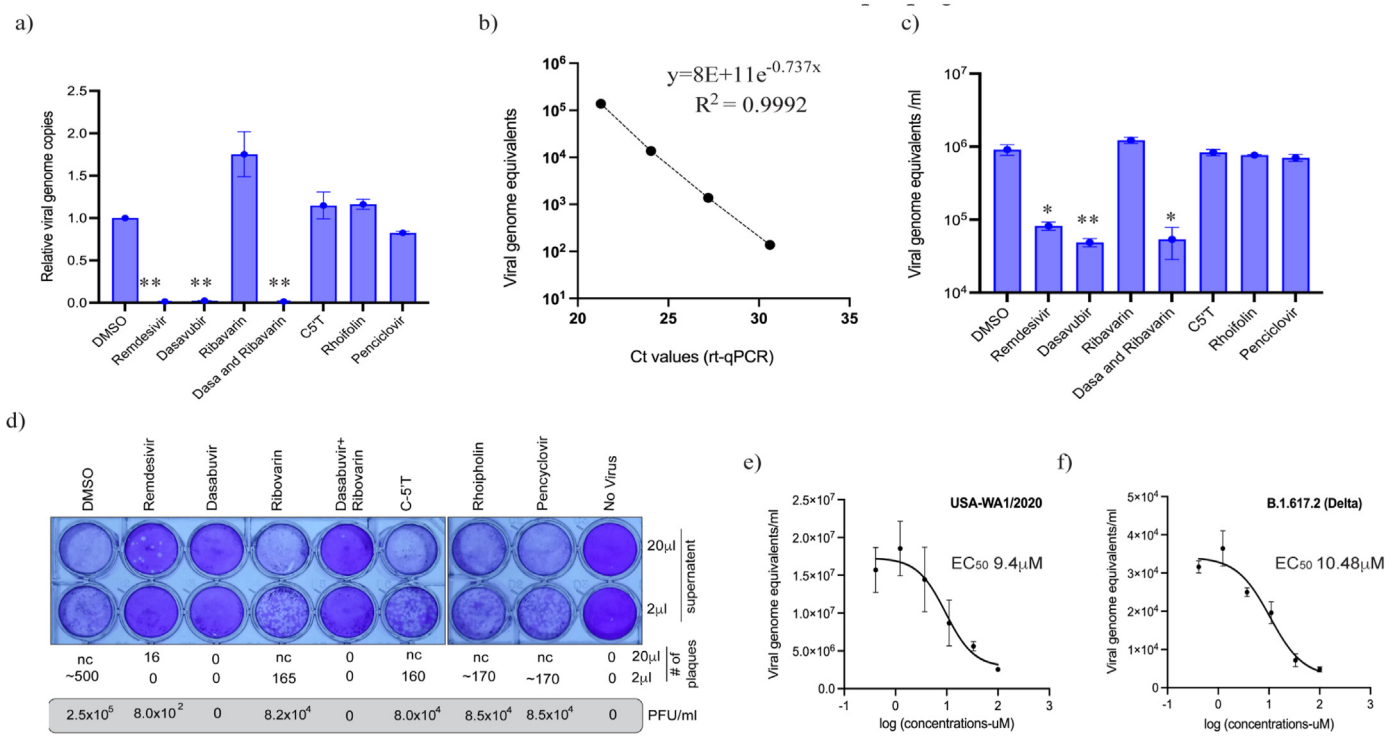

Fig. 6. Dasabuvir inhibits SARS-CoV-2 replication in Vero E6 cells. (A) Vero E6 cells were infected with USA-WA1/2020 and subsequently treated with DMSO (control) or 10 µM of the test compounds for 48h. a) Extracted RNA from the cells was used for the quantitation of intracellular SARS-CoV-2 genome through rt-PCR and plotted after normalization with the housekeeping gene. (B) Standard curve of known viral genome copies and Ct values for calculating the genome equivalents of SARS-CoV-2 in the supernatants. (C) Quantitation of cell-free SARS-CoV-2 genomes in the supernatants of compound treated cells through rt-PCR on extracted RNA. Genome copies per mL were calculated based on the Ct values using the standard curve. (D) Determination of infectious virus in the supernatant of treated cells through plaque assay. 20 µl and 2 µl of the supernatants from mock (no virus) and USA-WA1/2020 virus-infected cells and treated with different compounds were used for the plaque assay. Plaques were counted for determining the per mL plaque-forming units (PFU). nc = not countable. EC_{50} value of dasabuvir against SARS-CoV-2 was determined by measuring a reduction in the viral genome copies in the supernatant of (E) USA-WA1/2020 and (F) B.1.617.2 (Delta) infected cells following treatment with the varying amounts of dasabuvir. Statistical significance *, $p < 0.1$; and **, $p < 0.01$.

by infecting Vero E6 cells with SARS-CoV-2 variants USA-WA1/2020 and B.1.617.2) for 2h (37 °C and 5% CO_2), and subsequently treating the cells with DMSO (control) or the test compounds at (10 µM). After 3 days of incubation, viral RNA was extracted from the supernatant as well as the cells, and genomic SARS-CoV-2 RNA was quantified using rt-qPCR assay (Fig. 6). Intracellular genome copies of the virus in the cells treated with different compounds were determined relative to the copies in the DMSO treated cells (Fig. 6A). Cell-free genome copies of the virus in the supernatants were determined by using a standard curve generated with a known amount of SARS-CoV-2 genomic RNA (BEI Resources, NR-52285, Lot # 70033700) (Fig. 6B). We detected a significant decrease in the number of virus copies in the supernatants of cells treated with dasabuvir and its combination with Ribavirin. Remdesivir, showed a reduction in the viral genome copies in the supernatant, as expected (Fig. 6C). Next, the supernatants from compound-treated cells were evaluated for the presence of viable viruses through plaque assay (Fig. 6D). A monolayer of Vero E6 cells was inoculated with 20 µl and 2 µl of the collected supernatant for 2h and overlaid with 1.5% CMC containing DMEM medium. Seven days later, cell monolayers were fixed with formaldehyde and stained with crystal violet. Plaques were enumerated by direct visualization and PFUs values were reported as plaque-forming units per mL (PFU/mL) calculated through the Poisson distribution. Both dasabuvir-treated cells and dasabuvir/ribavirin-treated cells completely blocked the SARS-CoV-2 replication and propagation, as evident from the absence of plaques (Fig. 6D). Quantitative analysis of the antiviral activity of dasabuvir against SARS-CoV-2 replication was determined by calculating the half-maximal inhibitory concentration (EC_{50}). Vero E6 cells were infected with USA-WA1/2020 or B.1.617.2 virus (50 µL) and treated with varying concentrations of dasabuvir (serial dilutions ranging from 100 µM to 0.45 µM), along with untreated cells serving, as a control. After 48 h post-treatment, SARS-CoV-2 genome levels in the supernatants were quantified through the standard curve of Ct values and viral genome equivalents. The EC_{50} values of dasabuvir for WA1 and B.1.617.2 were determined by plotting the viral genome detected in the supernatants at each concentration using GraphPad. Dasabuvir treatment reduced the levels of SARS-CoV-2 in the supernatants of cells infected with WA1 as well as B.1.617.2 viruses (calculated EC_{50} values of 9.47 µM and 10.48 µM, for WA1 and B.1.617.2, respectively), indicating potential anti-SARS-CoV-2 activity of dasabuvir (Fig. 6E and F). Cytotoxicity of dasabuvir, determined previously (Stefanik et al., 2020) have a CC_{50} at ~100 µM on Vero cells and has moderate cytotoxicity. Taken together, these results demonstrate that dasabuvir has antiviral activity against SARS-CoV-2 and reduced SARS-CoV-2 replication efficiently in an *in-vitro* cell culture model.

3. Discussions

The emergence of highly pathogenic HCoVs, especially, SARS-CoV, MERS-CoV, and recently SARS-CoV-2, have threatened the public health security of almost all countries in the world. Although COVID-19 prophylactic vaccines currently authorized for use in the United States are effective against COVID-19 infection, the risk of SARS-CoV-2 infection in a fully vaccinated person can't be eliminated. Besides, new variants of SARS-CoV-2 circulating the globe have been reported to evade antibodies that neutralize the original SARS-CoV-2 variant, making them less effective as the new variants become dominant. Hence, an urgent

need remains to rapidly develop, and validate new and existing efficacious anti-SARS-CoV-2 drugs to limit the mortality and morbidity of severe COVID-19 infections.

Among other crucial viral proteins, SARS-CoV-2 encoded RdRp plays an essential role in the replication of the virus and is designated as a potential target for anti-SARS-CoV-2 drug development. Notably, the replication-transcription complex (RTC) of the human coronaviruses possesses exonuclease (ExoN) activity, which removes the erroneous nucleotides, thus poses a major obstacle in using nucleotides analogs (NAs) as an anti-virals for the coronaviruses (Smith et al., 2015; Agostini et al., 2018; Yan et al., 2021). Therefore, inhibitors capable of blocking the polymerase activity (RdRp) and the exonuclease activity could be better anti-virals for the coronaviruses. Our focus in this manuscript was to develop a cell-based assay to screen compounds capable of blocking the polymerase activity, owing to identical sequences among HCoVs and lack of human homolog, which may have an off-target effect. To demonstrate SARS-CoV-2 RdRp as a potential drug target, it was essential to have a stable, cell-based, target-specific functional assay that allows quantitative measurement of RdRp polymerase activity. Such an assay facilitates the determination of potential RdRp-specific inhibitors. Importantly, a cell-based assay stably expressing RdRp protein can help eliminate both cytotoxic and membrane-impermeable inhibitors. This shows the importance of a cell-based system for assaying the polymerase activity of SARS-CoV-2 RdRp.

While this manuscript was under preparation, Zhao et al. reported a cell-based CoV-RdRp-Gluc assay for the identification of SARS-CoV-2 RdRp inhibitors (Zhao et al., 2021). Culture supernatants of HEK293T cells transiently transfected with CoV-Gluc reporter along with nsp12, nsp7, nsp8, nsp10, and nsp14 expressing plasmids were subjected to Gluc activity assay. Although the assay successfully evaluated the efficacy of seven nucleotide analog compounds, however, the lack of steady RdRp expression adds variability in the gene expression and limits the immediate utilization of the developed assay in HTS applications. Here, we report the development of a simple and efficient HEK293 cell-based reporter assay system with steady RdRp protein expression for measuring the SARS-CoV-2 RdRp activity *in cells*. The system consists of the bicistronic SARS-CoV-2 RdRp reporter construct, p (+) RLuc-(−) UTR-FLuc, and Flag-tagged nsp5, 7, 8, and 12 plasmids. The FLuc gene expression represents the intracellular RdRp activity, whereas the RLuc gene expression serves as an internal control. This system allows rapid and quantitative measurement of SARS-CoV-2 RdRp activity in a cell-based format.

We quantified the accuracy of the system by screening known viral anti-polymerase drugs such as rhoifolin, penciclovir, ribavirin, dasabuvir, and cytidine-5′-triphosphate, as effective inhibitors of SARS-CoV-2 RdRp activity. Among them, rhoifolin, a flavonoid that was earlier shown to inhibit SARS-CoV $3CL^{Pro}$ (Jo et al., 2020), and penciclovir, a guanosine analog that is predicted to bind to SARS-CoV-2 RdRp via molecular docking studies (Grahl et al., 2021), did not significantly inhibit SARS-CoV-2 RdRp activity. Ribavirin, a broad-spectrum antiviral prevents viral RNA synthesis by depleting cellular guanosine triphosphate (Grahl et al., 2021). The incorporation of ribavirin triphosphate by RdRp has been shown to result in lethal viral mutagenesis (Eriksson et al., 1977; Pauly and Lauring, 2015). Our results illustrated that ribavirin only partially inhibited SARS-CoV-2 RdRp activity. Dasabuvir, a non-nucleoside HCV NS5B inhibitor and a derivative of benzothiadiazine (Gentile et al., 2014) suppressed SARS-CoV-2 RdRp activity at the conc. of 10 μM. Interestingly, ribavirin when used along with dasabuvir at 10 μM conc, did not alter the inhibitory effect of dasabuvir on SARS-CoV-2 RdRp activity. Taken together, we have developed a convenient, accurate, reproducible, and HTS-compatible reporter-based assay for rapid detection of inhibitors of anti-SARS CoV-2 RdRp activity without the need for culturing infectious SARS-CoV-2 virus. The described reporter assay system would be instrumental in screening and validating the in silico and virtually designed inhibitors and help expedite the identification of novel anti-COVID-19 therapeutic agents in the future.

4. Materials and methods

4.1. Cells, reagents, and antibodies

The human embryonic kidney HEK293 and Vero E6 cells were obtained from ATCC and maintained in Dulbecco's modified Eagle medium (DMEM) supplemented with 10% FBS (Atlanta Biologicals), 2 mM L-glutamine, 25 U/mL penicillin, and 25 μg/mL streptomycin. The cells were grown at 37 °C and 5% CO_2 in a humidified chamber. G418 and Hygromycin were purchased from InvivoGen (San Diego, CA, United States). Inhibitors, namely remdesivir (GS-5734), rhoifolin, ribavirin, dasabuvir, penciclovir, and cytidine-5′-triphosphate were purchased from Selleck Chemicals LLC (Houston, TX, United States) and stored as 10 mM in 100% dimethyl sulfoxide (DMSO) stock solutions at −20 °C. The final concentration of compounds was maintained constantly at 10 μM in the experiments unless mentioned. The mouse anti-Flag (M2, Sigma-Aldrich), and mouse anti-GAPDH (G8140, US Biological, Salem MA) antibodies were used in this study.

4.2. Viruses

USA-WA1/2020 and B.1.617.2 strains were obtained from BEI Resources and propagated in Vero E6 cells by infecting the cell monolayer with the virus for 2 h at 37 °C. The unattached virus was removed by washing followed by the addition of fresh medium. After 72phi, the supernatant was harvested, and the cell debris was removed by centrifugation. The virus was aliquoted and stored at −80 °C until further use. Viral copies in the harvested supernatant were quantified by Reverse Transcriptase qPCR (qRT-PCR) by using standard SARS-CoV-2 genomic RNA with known amounts of SARS-CoV-2 (BEI Resources). SARS-CoV-2 infection assays were performed in the BSL-3 containment facility of the University of Nevada, Reno.

4.3. Establishment of the stable cell lines

Permissive HEK293 cells were transfected with RdRp-luciferase reporter and pcDNA3.1. HA or Flag-tagged nsp5,7,8,12 constructs (synthesized from Genscript. Inc.) in a 12-well plate, using metafectene and lipofectamine reagent, respectively, as per manufacturer's instructions. After 24h, cells were selected using 250 μg/mL G418 (for 293/RdRp cell lines) or 250 μg/mL G418 and 25 μg/mL hygromycin (for 293/RdRp-nsp5,7,8,12-Flag cell lines). After 3 weeks of selection, expanded clones were examined for the expression of Flag-tagged nsp12 (RdRp) by Western blot using an anti-Flag antibody. The same blot was also stained with anti-GAPDH to serve as the loading control. *Firefly* and *Renilla* luciferase reporter gene expression in the cells was measured with a Dual-Luciferase Assay System (Promega Corporation, Madison, WI, United States) according to the manufacturer's instructions. Briefly, 150,000 cells per well were plated in a 12-well plate. For compound treatment, cells were treated with selective inhibitors at a final conc. of 10 μM or DMSO alone (control) for 48h. Cells were then lysed in 100 μL of 1X passive lysis buffer and incubated at RT for 15 min to ensure complete lysis. The lysate was transferred to a 96-well microplate, followed by the addition of 100 μL of the *firefly* luciferase reagent (LARII) with a 10-s equilibration time and measurement of luminescence. Next, 100 μL of the Renilla luciferase reagent (Stop & Glo) for *firefly* luminescence quenching was added with a 10-s equilibration time and measurement of luminescence. The relative activity of RdRp polymerase was determined by normalizing the level of *firefly* luciferase activity (FLuc) against that of *renilla* luciferase activity (RLuc), FLuc/RLuc.

4.4. Immunoprecipitation and Western blotting

For immunoprecipitation, nearly 5×10^6 cells were harvested and washed with cold 1X PBS, lysed in RIPA lysis buffer (1% NP-40, 50 mM Tris [pH 7.5], 1 mM EDTA [pH 8.0], and 150 mM NaCl) supplemented

with protease inhibitors (1 mM phenylmethylsulfonyl fluoride, 1 μg/mL aprotinin, 1 μg/mL pepstatin, 1 μg/mL sodium fluoride, and 1 μg/mL leupeptin), and incubated on ice for 30 min. Cell lysates were sonicated with a probe sonicator and cell debris was removed by centrifugation (12,000 rpm, 10 min at 4 °C). The lysates were pre-cleared with protein A + G conjugated sepharose beads (30 min at 4 °C). Approx. 5% of the lysate was saved as an input sample and the remaining lysate was incubated (while rotating) with an anti-flag antibody overnight at 4 °C. Immune complexes were captured by incubating with 35 μL of protein A + G sepharose beads for 2h at 4 °C. The beads-bound immune complexes (IP samples) were collected by centrifugation (2000 rpm, 2 min at 4 °C), followed by washing with ice-cold RIPA buffer (2X). The input samples and the IP samples were resuspended in 45 μL of SDS-PAGE loading buffer and denatured at 95 °C for 5 min, resolved by SDS-PAGE and western blotted onto a 0.45 μM nitrocellulose membrane using standard protocols (Bio-Rad Laboratories, Hercules, CA, United States). Proteins of interest were detected by incubating the membrane with specific antibodies, followed by incubation with appropriate infrared-dye-tagged secondary antibodies (IR-Dye680/800) and scanning with an Odyssey infrared scanner (Li-COR Biosciences, Lincoln, NE, United States).

4.5. RNA extraction and RT-qPCR

Relative expressions of FLuc and RLuc gene transcripts in cells were measured by real-time reverse transcription PCR (RT-qPCR). Total mRNA from the cells was extracted using Trizol reagent (Thermo Fisher Scientific, Waltham, MA, United States) according to the manufacturer's recommendation. The cDNA was made using a high-capacity RNA-to-cDNA Kit (Thermo Fisher Scientific) and amplified on the Bio-Rad CFX Connect RT-qPCR detection system (Bio-Rad). Each amplification reaction was performed in a 20 μL volume containing 10 μL of SYBR Green Universal master mix (Bio-Rad), 2.5 μL each of forward and reverse primers (2 μM) targeting corresponding genes, and 5 μL of cDNA or water. Primers used in this study are: **FLuc-F** (5′-ATC GAA GGA CTC TGG CAC AA-3′), **FLuc-R** (5′-CCT ACC GTG GTG TTC GTT TC-3′), **RLuc-F** (5′-AGT GGT GGG CCA GAT GTA AA-3′), and **RLuc-R** (5′-CGC GCT ACT GGC TCA ATA TG-3′). The specificity of amplification was assessed by analyzing the melting curve. The relative mRNA expression level of each target gene (FLuc and RLuc) was normalized to the corresponding beta-actin expression level, and the fold change was calculated using the $\Delta\Delta C_T$ method with respect to cells expressing RdRp reporter plasmid.

For relative viral genome quantification post-infection and compound treatment, control or USA-WA1/2020 virus was added onto the Vero E6 cells plated in a 24-well plate (100,000 cells per well) for 2h (37 °C and 5% CO_2). Post-infection, the virus-containing medium was replaced with a 1 mL fresh medium containing either DMSO (control) or compounds (10 μM). The cells were treated with compounds for 72h at 37 °C and 5% CO_2. For the detection of viral genomic RNA through qRT-PCR, supernatant from control or compound-treated Vero E6 cells (for intact viral genomic RNA) or from treated cells (for infectious viral genomic RNA) were subjected for total RNA extraction using Trizol reagent (Invitrogen, Carlsbad, CA, USA) via direct-zol RNA extraction kit (Zymo Research), according to the manufacturer's recommendation. An aliquot of extracted total RNA (5 μL) was used for the relative quantification of viral genomic copies using TaqPath and N1 primer-probe set in a qRT-PCR assay (Thermo Fisher Scientific, Waltham, MA, USA).

4.6. Cell toxicity assay or Methyl Thiazolyl tetrazolium (MTT) assay

Cell toxicity due to the compound treatment was determined using the standard colorimetric MTT [3-(4,5-dimethylthiazol-2-yl)-2,5-diphenyltetrazolium bromide] assay (Thermo Fisher Scientific) according to the manufacturer's instructions. Briefly, 5000 cells resuspended in the complete DMEM medium were seeded in a costar 96-well microplate and grown overnight. The next day, cells were washed with 1X PBS and treated by adding 100 μL of MTT solution (0.5 mg/mL) to each well, followed by incubation at 37 °C for 4h. The culture medium (100 μL) was used as a negative control (blank). After 4h, when intracellular purple formazan crystals were visible under the microscope, MTT solution was removed and replaced with 50 μL of solubilizing DMSO solution. Cells were incubated at RT for 30 min to dissolve the purple formazan crystals. The absorbance was measured on a microplate reader at a wavelength of 570 nm. The background absorbance produced by wells containing medium only (Abs_{blank}) was subtracted from all wells, and the percent viable cells were calculated using the equation: %viable cells = [(Abs_{sample}-Abs_{blank})/($Abs_{control}$-Abs_{blank})] *100.

4.7. Dose-Response assays

Vero E6 cells were seeded at 100,000 cells per well in a 24-well microplate and allowed to attach for 2h. The cells were infected with USA-WA1/2020 or B.1.617.2 variant for 2h, followed by treatment with dasabuvir at concentrations 100, 33, 11, 3.7, 1.23, and 0.41 μM, in duplicate. After 48 h of incubation at 37 °C with 5% CO_2, the supernatant was collected and a fraction (100 μL) was used for RNA extraction and rt-qPCR (reverse transcriptase-PCR) to quantify the amounts of SARS-CoV-2 in the supernatant. Another fraction of the supernatant was used for the detection of infectious SARS-CoV-2 through the enumeration of plaque-forming units described below. The absolute half-maximal inhibitory concentrations (EC_{50}) of dasabuvir for SARS-CoV-2, USA-WA1/2020, and B.1.617.2 were calculated, based on the amounts of residual virus in the supernatant at each concentration, using the Graphpad Prism™.

4.8. Plaque assay

Vero E6 cells (100,000 cells/well) in 1 mL medium were seeded in a 24-well culture plate for 2h (37 °C and 5% CO_2). Next, 20 μL and 2 μL (10-fold dilution) of virus-containing supernatant (post compound treatment) were added to the cells, and the cell plate was incubated for 2 h (37 °C with 5% CO_2), followed by the replacement of the medium with 1.5% CMC overlay medium. After 7 days of incubation, the overlay medium was replaced with 4% paraformaldehyde solution (500 μL), and the cells were incubated at room temperature for 30 min. Fixed cells were stained with 0.2% crystal violet solution in 20% ethanol (500 μL) at room temperature for 30 min with a gentle rocking after every 10 min. The staining solution was removed, and cells were washed with sterile distilled water (thrice). The plate was inverted and left for drying on an absorbent pad for 1–2h. Plaques appeared as clear circles in the purple monolayer of cells (used negative control with no clear circles as reference). For each well, the number of plaques for that dilution was counted, and plaque-forming units (PFU per mL) were calculated using the equation-

PFU/mL = average number of plaques/[dilution factor of the well x volume of inoculum per plate]

4.9. Calculation of Z-Factor and Z′-Factor

To evaluate the quality and reproducibility of the screening assay, screening window coefficients, Z- and Z′-factor values were calculated as described previously. Briefly, 50,000 cells per well were plated in a 24-well plate for each group as follows: (1) Control group = cells expressing RdRp reporter plasmid and pcDNA3.1 (control vector), $n = 24$ wells, treated with 0.025% DMSO; (2) Positive group = cells expressing RdRp reporter plasmid and Flag-tagged nsp5, 7, 8, 12 plasmid, $n = 24$ wells, treated with 0.025% DMSO; and (3) Inhibitor group = cells with RdRp reporter plasmid and Flag-tagged nsp5, 7, 8, 12 plasmid, $n = 24$ wells, treated with 10 μM remdesivir. Post 48h, cells were lysed in 100 μL of 1X passive lysis buffer and subjected to dual-luciferase reporter assay, as mentioned in Section 2.3. The relative activity of RdRp was determined by normalizing the level of FLuc to that of RLuc (FLuc/RLuc). Z-factor

was calculated using the equation: Z-factor = 1 − [(3SD$_{Control}$ + 3SD$_{Positive}$)/|mean$_{Control}$ − mean$_{Positive}$|], and Z′-factor was calculated using the equation: Z′-factor = 1 − [(3SD$_{Inhibitor}$ + 3SD$_{Positive}$)/|mean$_{Inhibitor}$ − mean$_{Positive}$|], where SD (the standard deviation) and mean values correspond to the relative FLuc activity obtained from each group.

4.10. Statistical analyses

All the experiments were performed three times, and the data is presented as the mean of a triplicate. The error bars represent the standard deviation across three independent experiments. Statistical analyses were performed using Prism 8.0 software (GraphPad Inc.). The p-values were calculated using two-way analysis of variance (ANOVA) tests, and the *p*-value cut-offs for statistical significance were *, $p < 0.1$; and **, $p < 0.01$.

Author contributions

Timsy Uppal: Methodology, Investigation, and writing; † **Kai Tuffo:** Investigation; **Svetlana Khaiboullina:** Conceptualization and Methodology; † **Sivani Reganti:** Investigation; **Mark Pandori:** Supervision; **and Subhash C. Verma:** Conceptualization, Methodology, Writing, Supervision, Project administration, and Funding acquisition.

Declaration of competing interest

The authors declare no competing interest.

Acknowledgments

SARS-CoV-2 viruses USA-WA1/2020 (NR-52281) and B.1.617.2 (NR-55611) were obtained from BEI Resources, NIAID, and NIH. The study was carried out with institutional resources and support from the Department of Microbiology and Immunology, University of Nevada, Reno School of Medicine, Reno, United States. T.U. was partly supported by an award from the NIGMS, NIH under grant number U54 GM104944.

References

Agostini, M. L., Andres, E. L., Sims, A. C., Graham, R. L., Sheahan, T. P., Lu, X., Smith, E. C., Case, J. B., Feng, J. Y., Jordan, R., Ray, A. S., Cihlar, T., Siegel, D., Mackman, R. L., Clarke, M. O., Baric, R. S., & Denison, M. R. (2018). Coronavirus susceptibility to the antiviral remdesivir (GS-5734) is mediated by the viral polymerase and the proofreading exoribonuclease. *mBio, 9*(2).

Anastassopoulou, C., Hatziantoniou, S., Boufidou, F., Patrinos, G. P., & Tsakris, A. (2022). The role of oral antivirals for COVID-19 treatment in shaping the pandemic landscape. *J. Personalized Med., 12*(3).

Chien, M., Anderson, T. K., Jockusch, S., Tao, C., Li, X., Kumar, S., Russo, J. J., Kirchdoerfer, R. N., & Ju, J. (2020). Nucleotide analogues as inhibitors of SARS-CoV-2 polymerase, a key drug target for COVID-19. *J. Proteome Res., 19*(11), 4690–4697.

Dhama, K., Patel, S. K., Sharun, K., Pathak, M., Tiwari, R., Yatoo, M. I., Malik, Y. S., Sah, R., Rabaan, A. A., Panwar, P. K., Singh, K. P., Michalak, I., Chaicumpa, W., Martinez-Pulgarin, D. F., Bonilla-Aldana, D. K., & Rodriguez-Morales, A. J. (2020). SARS-CoV-2 jumping the species barrier: zoonotic lessons from SARS, MERS and recent advances to combat this pandemic virus. *Trav. Med. Infect. Dis., 37*, Article 101830.

Eriksson, B., Helgstrand, E., Johansson, N. G., Larsson, A., Misiorny, A., Norén, J. O., Philipson, L., Stenberg, K., Stening, G., Stridh, S., & Oberg, B. (1977). Inhibition of influenza virus ribonucleic acid polymerase by ribavirin triphosphate. *Antimicrob. Agents Chemother., 11*(6), 946–951.

Gao, Y., Yan, L., Huang, Y., Liu, F., Zhao, Y., Cao, L., Wang, T., Sun, Q., Ming, Z., Zhang, L., Ge, J., Zheng, L., Zhang, Y., Wang, H., Zhu, Y., Zhu, C., Hu, T., Hua, T., Zhang, B., Yang, X., Li, J., Yang, H., Liu, Z., Xu, W., Guddat, L. W., Wang, Q., Lou, Z., & Rao, Z. (2020). Structure of the RNA-dependent RNA polymerase from COVID-19 virus. *Science, 368*(6492), 779–782.

Gentile, I., Buonomo, A. R., & Borgia, G. (2014). Dasabuvir: a non-nucleoside inhibitor of NS5B for the treatment of hepatitis C virus infection. *Rev. Recent Clin. Trials, 9*(2), 115–123.

Gordon, C. J., Tchesnokov, E. P., Feng, J. Y., Porter, D. P., & Götte, M. (2020). The antiviral compound remdesivir potently inhibits RNA-dependent RNA polymerase from Middle East respiratory syndrome coronavirus. *J. Biol. Chem., 295*(15), 4773–4779.

Grahl, M. V. C., Alcará, A. M., Perin, A. P. A., Moro, C. F., Pinto, É. S. M., Feltes, B. C., Ghilardi, I. M., Rodrigues, F. V. F., Dorn, M., da Costa, J. C., Norberto de Souza, O., & Ligabue-Braun, R. (2021). Evaluation of drug repositioning by molecular docking of pharmaceutical resources available in the Brazilian healthcare system against SARS-CoV-2. *Inform. Med. Unlocked, 23*, Article 100539.

Hillen, H. S., Kokic, G., Farnung, L., Dienemann, C., Tegunov, D., & Cramer, P. (2020). Structure of replicating SARS-CoV-2 polymerase. *Nature, 584*(7819), 154–156.

Jo, S., Kim, S., Shin, D. H., & Kim, M. S. (2020). Inhibition of SARS-CoV 3CL protease by flavonoids. *J. Enzym. Inhib. Med. Chem., 35*(1), 145–151.

Kabinger, F., Stiller, C., Schmitzová, J., Dienemann, C., Kokic, G., Hillen, H. S., Höbartner, C., & Cramer, P. (2021). Mechanism of molnupiravir-induced SARS-CoV-2 mutagenesis. *Nat. Struct. Mol. Biol., 28*(9), 740–746.

Kokic, G., Hillen, H. S., Tegunov, D., Dienemann, C., Seitz, F., Schmitzova, J., Farnung, L., Siewert, A., Höbartner, C., & Cramer, P. (2021). Mechanism of SARS-CoV-2 polymerase stalling by remdesivir. *Nat. Commun., 12*(1), 279.

Lee, J. C., Tseng, C. K., Chen, K. J., Huang, K. J., Lin, C. K., & Lin, Y. T. (2010). A cell-based reporter assay for inhibitor screening of hepatitis C virus RNA-dependent RNA polymerase. *Anal. Biochem., 403*(1–2), 52–62.

Liu, X.-h., Zhang, X., Lu, Z.-h., Zhu, Y.-s., & Wang, T. (2021). Potential molecular targets of nonstructural proteins for the development of antiviral drugs against SARS-CoV-2 infection. *Biomed. Pharmacother., 133*, Article 111035.

Min, J. S., Kim, G. W., Kwon, S., & Jin, Y. H. (2020). A cell-based reporter assay for screening inhibitors of MERS coronavirus RNA-dependent RNA polymerase activity. *J. Clin. Med., 9*(8).

Mokhtari, T., Hassani, F., Ghaffari, N., Ebrahimi, B., Yarahmadi, A., & Hassanzadeh, G. (2020). COVID-19 and multiorgan failure: a narrative review on potential mechanisms. *J. Mol. Histol., 51*(6), 613–628.

Naqvi, A. A. T., Fatima, K., Mohammad, T., Fatima, U., Singh, I. K., Singh, A., Atif, S. M., Hariprasad, G., Hasan, G. M., & Hassan, M. I. (2020). Insights into SARS-CoV-2 genome, structure, evolution, pathogenesis and therapies: structural genomics approach. *Biochim. Biophys. Acta, Mol. Basis Dis., 1866*(10), Article 165878.

Owen, D. R., Allerton, C. M. N., Anderson, A. S., Aschenbrenner, L., Avery, M., Berritt, S., Boras, B., Cardin, R. D., Carlo, A., Coffman, K. J., Dantonio, A., Di, L., Eng, H., Ferre, R., Gajiwala, K. S., Gibson, S. A., Greasley, S. E., Hurst, B. L., Kadar, E. P., Kalgutkar, A. S., Lee, J. C., Lee, J., Liu, W., Mason, S. W., Noell, S., Novak, J. J., Obach, R. S., Ogilvie, K., Patel, N. C., Pettersson, M., Rai, D. K., Reese, M. R., Sammons, M. F., Sathish, J. G., Singh, R. S. P., Steppan, C. M., Stewart, A. E., Tuttle, J. B., Updyke, L., Verhoest, P. R., Wei, L., Yang, Q., & Zhu, Y. (2021). An oral SARS-CoV-2 M^{pro} inhibitor clinical candidate for the treatment of COVID-19. *Science, 374*(6575), 1586–1593.

Pauly, M. D., & Lauring, A. S. (2015). Effective lethal mutagenesis of influenza virus by three nucleoside analogs. *J. Virol., 89*(7), 3584–3597.

Romano, M., Ruggiero, A., Squeglia, F., Maga, G., & Berisio, R. (2020). A structural view of SARS-CoV-2 RNA replication machinery: RNA synthesis, proofreading and final capping. *Cells, 9*(5).

Smith, E. C., Case, J. B., Blanc, H., Isakov, O., Shomron, N., Vignuzzi, M., & Denison, M. R. (2015). Mutations in coronavirus nonstructural protein 10 decrease virus replication fidelity. *J. Virol., 89*(12), 6418–6426.

Stefanik, M., Valdes, J. J., Ezebuo, F. C., Haviernik, J., Uzochukwu, I. C., Fojtikova, M., Salat, J., Eyer, L., & Ruzek, D. (2020). FDA-approved drugs efavirenz, tipranavir, and dasabuvir inhibit replication of multiple flaviviruses in Vero cells. *Microorganisms, 8*(4).

Sui, Y., & Wu, Z. (2007). Alternative statistical parameter for high-throughput screening assay quality assessment. *J. Biomol. Screen, 12*(2), 229–234.

Vicenti, I., Zazzi, M., & Saladini, F. (2021). SARS-CoV-2 RNA-dependent RNA polymerase as a therapeutic target for COVID-19. *Expert Opin. Ther. Pat., 31*(4), 325–337.

Wang, C., Horby, P. W., Hayden, F. G., & Gao, G. F. (2020). A novel coronavirus outbreak of global health concern. *Lancet, 395*(10223), 470–473.

Williamson, B. N., Feldmann, F., Schwarz, B., Meade-White, K., Porter, D. P., Schulz, J., van Doremalen, N., Leighton, I., Yinda, C. K., Pérez-Pérez, L., Okumura, A., Lovaglio, J., Hanley, P. W., Saturday, G., Bosio, C. M., Anzick, S., Barbian, K., Cihlar, T., Martens, C., Scott, D. P., Munster, V. J., & de Wit, E. (2020). Clinical benefit of remdesivir in rhesus macaques infected with SARS-CoV-2. *Nature, 585*(7824), 273–276.

Yan, L., Yang, Y., Li, M., Zhang, Y., Zheng, L., Ge, J., Huang, Y. C., Liu, Z., Wang, T., Gao, S., Zhang, R., Huang, Y. Y., Guddat, L. W., Gao, Y., Rao, Z., & Lou, Z. (2021). Coupling of N7-methyltransferase and 3'-5' exoribonuclease with SARS-CoV-2 polymerase reveals mechanisms for capping and proofreading. *Cell, 184*(13), 3474–3485. e3411.

Zhao, J., Guo, S., Yi, D., Li, Q., Ma, L., Zhang, Y., Wang, J., Li, X., Guo, F., Lin, R., Liang, C., Liu, Z., & Cen, S. (2021). A cell-based assay to discover inhibitors of SARS-CoV-2 RNA dependent RNA polymerase. *Antivir. Res., 190*, Article 105078.